



# Taking a color photo: A homozygous 25-bp deletion in Bace2 may cause brown-and-white coat color in giant pandas

Dengfeng Guan<sup>a,b,1</sup>, Shuyan Sun<sup>a,c,1</sup>, Lingyun Song<sup>a,c</sup>, Pengpeng Zhao<sup>d</sup>, Yonggang Nie<sup>a,c</sup>, Xin Huang<sup>a,c</sup>, Wenliang Zhou<sup>e</sup>, Li Yan<sup>a</sup>, Yinghu Lei<sup>d</sup>, Yibo Hu<sup>a,c,2</sup> , and Fuwen Wei<sup>a,b,c,e,2</sup>

Edited by Sean Carroll, Howard Hughes Medical Institute, Chevy Chase, MD; received October 9, 2023; accepted December 30, 2023

Brown-and-white giant pandas (hereafter brown pandas) are distinct coat color mutants found exclusively in the Qinling Mountains, Shaanxi, China. However, its genetic mechanism has remained unclear since their discovery in 1985. Here, we identified the genetic basis for this coat color variation using a combination of field ecological data, population genomic data, and a CRISPR-Cas9 knockout mouse model. We de novo assembled a long-read-based giant panda genome and resequenced the genomes of 35 giant pandas, including two brown pandas and two family trios associated with a brown panda. We identified a homozygous 25-bp deletion in the first exon of *Bace2*, a gene encoding amyloid precursor protein cleaving enzyme, as the most likely genetic basis for brown-and-white coat color. This deletion was further validated using PCR and Sanger sequencing of another 192 black giant pandas and CRISPR-Cas9 edited knockout mice. Our investigation revealed that this mutation reduced the number and size of melanosomes of the hairs in knockout mice and possibly in the brown panda, further leading to the hypopigmentation. These findings provide unique insights into the genetic basis of coat color variation in wild animals.

coat color variation | brown giant panda | population genomics | Bace2 | melanosome

Coat color variation has substantial adaptive and cultural value in mammals (1-4). This trait is directly determined by the ratio of eumelanin to pheomelanin, as well as the density and distribution of melanosomes in hair (5). These factors are under complex regulation by hundreds of genes that influence various aspects of melanogenesis, including melanocyte proliferation and migration, melanin synthesis, and melanosome biogenesis and transfer (6).

The giant panda (Ailuropoda melanoleuca), one of the most charismatic flagship species, is characterized by its striking black-and-white coat color (hereafter black panda); however, the discovery of brown pandas in the Qinling Mountains, Shaanxi Province, China, challenges the conventional belief that the panda can never have a color photo. These brown pandas are exceedingly rare, which has undoubtedly made them the treasures of national treasures. Since the first brown panda was found in 1985, eleven records have been reported by official news or personal communications (SI Appendix, Fig. S1 and Table S1), of which seven cases have been confirmed with photographs or entities: three from Foping County, two from Yangxian, one from Taibai, and one from Zhouzhi. All brown pandas were found exclusively in the Qinling Mountains, indicating that they are endemic to this region. The first recorded brown panda, a female named Dandan, was rescued to Xi'an Zoo from the Foping Nature Reserve (FNR) in 1985. She later mated with a black panda, Wanwan, and gave birth to a male black panda, Qinqin, in captivity. Dandan passed away in 2000, while Qinqin followed in 2006, leaving no offspring behind. In 2009, a male brown panda cub, Qizai, was rescued from the FNR and is currently the only brown panda living in captivity. The discovery of brown pandas has aroused considerable public attention regarding the formation of their unique coat color (7). The recurring instances of brown pandas imply that this trait may be inheritable. However, to date, the genetic basis underlying the brown-and-white coat color remains unclear.

In this study, we established two family trios associated with the brown panda Qizai and determined the Mendelian inheritance pattern of brown coat color, using ecological and genetic data from our long-term study of wild giant pandas in the FNR. We identified the candidate mutation, a 25-bp deletion in Bace2 gene, as the most likely genetic basis of brown pandas, by using long-read based chromosome-level genome assembly, whole genome resequencing data of population and two family trios of a brown panda, and confirmed it with RNA-seq data, large-scale population Sanger sequencing and a CRISPR-Cas9 knockout mouse model. Furthermore, we explored the cellular mechanisms underlying the brown coat color based on the analysis of microscopy and transmission electron microscopy (TEM). This study not only provides insights into the genetic basis of coat

## **Significance**

Coat color variation is one of the most diverse traits in wild animals. The giant pandas can have a color photo because of the occurrence of brown pandas. However, the genetic basis of the brown-and-white coat color has remained elusive in the past about four decades. We identified a homozygous 25-bp deletion in the first exon of Bace2 as the most likely genetic basis for brown-and-white coat color variation in giant pandas. Our study provides unique insights into the genetic basis of coat color variation in wild animals and will guide scientific breeding of the rare brown pandas.

Author affiliations: <sup>a</sup>Key Laboratory of Animal Ecology and Conservation Biology, Institute of Zoology, Chinese Academy of Sciences, Beijing 100101, China; <sup>b</sup>Jiangxi Provincial Key Laboratory of Conservation Biology, Jiangxi Agricultural University, Nanchang 330045, China; <sup>1</sup>University of Chinese Academy of Sciences, Beijing 100049, China; <sup>d</sup>Shaanxi (Louguantai) Rescue and Breeding Center for Rare Wildlife, Xi'an 710402, China; and <sup>e</sup>Center for Evolution and Conservation Biology, Southern Marine Science and Engineering Guangdong Laboratory (Guangzhou), Guangzhou 511458, China

Author contributions: F.W. and Y.H. conceived and supervised the research; Y.H., F.W., Y.N., W.Z., P.Z., Y.L., D.G. and L.Y. collected the panda samples; S.S. and L.S. collected the mouse samples; Y.H., W.Z., L.Y., S.S., L.S. and D.G. performed the experiments; D.G. and X.H. analyzed the data; Y.H., W.Z., Y.N., D.G., S.S. and F.W. discussed the results; and D.G., Y.H., F.W., S.S., W.Z., and Y.N. wrote and edited the paper.

The authors declare no competing interest.

This article is a PNAS Direct Submission.

Copyright © 2024 the Author(s). Published by PNAS. This article is distributed under Creative Commons Attribution-NonCommercial-NoDerivatives License 4.0 (CC BY-NC-ND).

<sup>1</sup>D.G. and S.S. contributed equally to this work.

<sup>2</sup>To whom correspondence may be addressed. Email: ybhu@ioz.ac.cn or weifw@ioz.ac.cn.

This article contains supporting information online at https://www.pnas.org/lookup/suppl/doi:10.1073/pnas. 2317430121/-/DCSupplemental.

Published March 4, 2024.

color variation in brown pandas and even in wild animals but also would guide scientific breeding of the rare brown pandas.

## **Results**

Phenotype of Hairs from Brown and Black Pandas. The black pandas are covered in black-and-white fur, while the brown panda has brown-and-white fur (Fig. 1A). To characterize the hair features of black and brown pandas, we collected hairs of the left forelimb and left hindlimb from three black pandas and one brown panda (Qizai) in captivity. Microscopic scan of brown and black hairs showed that the brown hairs might have fewer melanosomes than the black ones (Fig. 1B). To better understand how melanosomes varied in terms of number and size, we performed TEM examination of the highly pigmented middle part of the black and brown hairs and found that melanosomes of the black hairs showed nearly circular shape in the transverse sections and elongated oval shape in the longitudinal sections, while melanosomes of the brown hairs demonstrated smaller circular/oval or irregular shape in both the transverse and longitudinal sections (Fig. 1 C and D). Statistical analyses revealed that the brown hairs had 22% fewer melanosomes (P < 0.05) and 55% smaller melanosomes (P < 0.001) on average than the black hairs (Fig. 1 *E* and *F* and Dataset S1). Additionally,

the brown hairs exhibited extensive aberrant melanosomes where melanin was sparsely distributed, resembling the case in *Pmel* knockout mice (8).

Mendelian Inheritance Pattern of the Brown-and-White Coat Color. To elucidate the genetic architecture of brown coat color, we

first investigated the inheritance pattern of the brown coat color and then performed genome-wide variant screening to capture all potential variants associated with this phenotype based on the identified inheritance pattern and its geographical distribution.

We extracted DNA from fresh feces or blood samples and performed maternal and paternal recognition using microsatellite genotypes (Dataset S2). Our genetic analysis confirmed that the fresh feces collected at Qizai's rescue site of FNR was from his mother, Niuniu, a collared wild female black panda (9–11) (SI Appendix, Fig. S2). Furthermore, we identified a collared male black panda named Xiyue as Qizai's biological father based on the microsatellite genotyping of all 157 panda individuals in our study area (Fig. 2A, B1 family). Our field observation and genetic analysis found that Niuniu had successfully mated with another collared male black panda named Diandian in 2012 and gave birth to a male black panda, Longbao (Fig. 2A). Later in captivity, a female black panda, Zhuzhu, gave birth to a male black panda

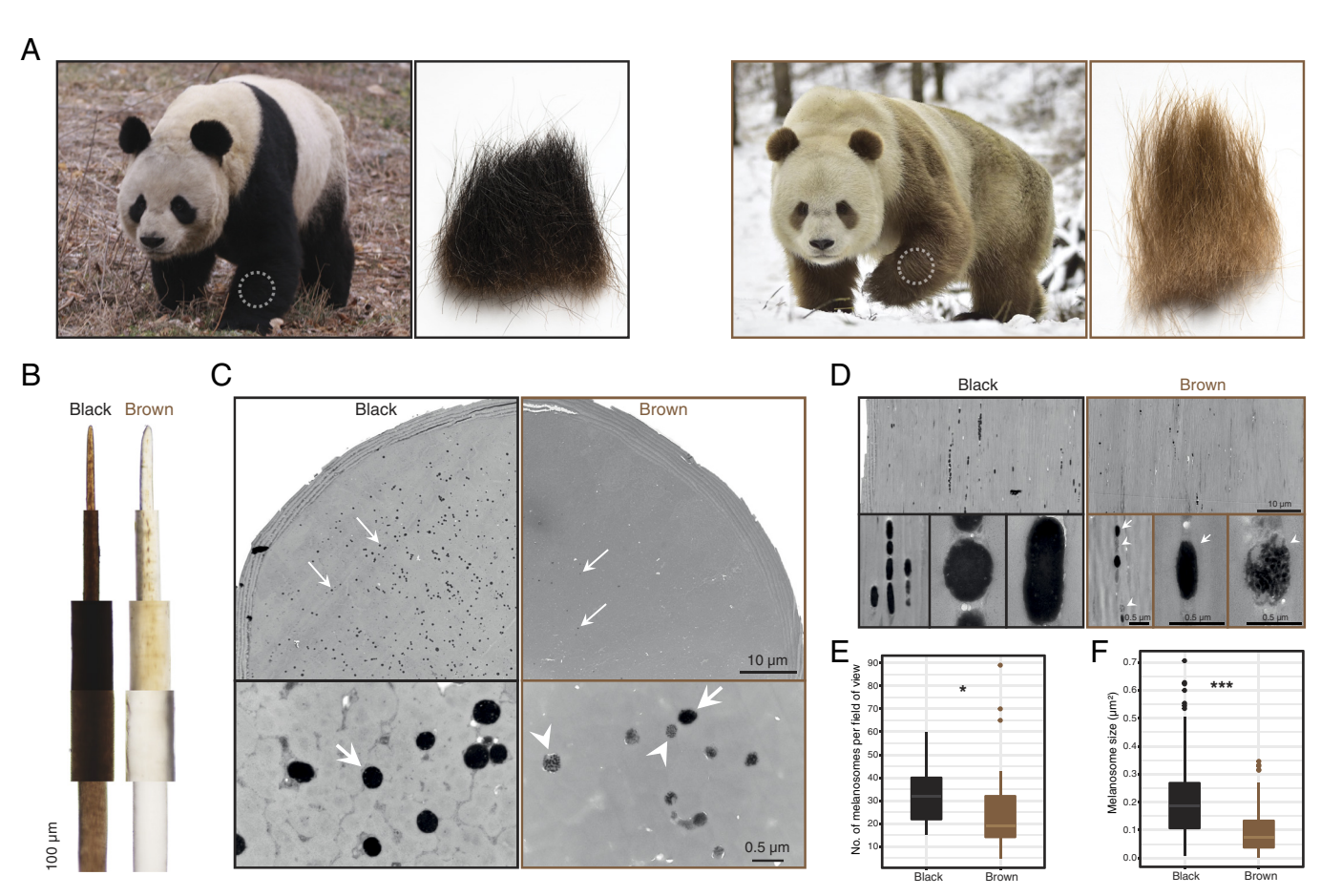


Fig. 1. Phenotypes of hairs of black and brown pandas. (A) Images of hairs of a black panda and a brown panda (Qizai). (B) Sequential microscopic photographs from hair tip (Upper) to near root (Lower) of black (Left) and brown (Right) hairs. (C) TEM images of a transverse section of hairs from black (Upper Left and Lower Left micrographs) and brown pandas (Upper Right micrographs). Upper two micrographs represent  $\frac{1}{4}$  hair shaft, melanosomes are marked by white arrows. The Lower two micrographs are partially upscaled transverse sections, and melanosomes are indicated by white arrows, while some aberrant ones are marked by white arrowheads. (D) TEM images of a longitudinal section of hairs from black (Upper Left and Lower Left micrographs) and brown pandas (Upper Right and Lower Right micrographs). Lower Left images consist of three micrographs in the same scale corresponding to the Right ones. In micrographs of the brown hair, melanosomes are indicated by white arrows, while some aberrant ones are marked by white arrowheads. (E) Melanosome number per view field of hair of a black panda and a brown panda (33 fields for the black panda, 38 fields for the brown panda; black: 33.39  $\pm$  12.18, brown: 25.89  $\pm$  17.99, mean  $\pm$  SD) (\*P < 0.05, one-sided Welch's t test). (F) Melanosome size per se in hair (n = 1,049 melanosomes for the black panda, and n = 233 melanosomes for the brown panda; black: 0.19  $\pm$  0.11  $\pm$  0

Qinhua in 2020, and paternal identification based on microsatellite genotyping confirmed that Qinhua's father is the brown panda Qizai (Fig. 2A, B2 family). As a result, we established two family trios associated with the brown panda Qizai, which was further confirmed by kinship analysis based on population single nucleotide polymorphism (SNP) data (SI Appendix, Fig. S3 and Dataset S3). By integrating with a known family trio of the brown panda Dandan (Fig. 2A, B3 family), we identified three family trios associated with brown pandas. Based on the pedigree, we conclude that the brown coat color is governed by autosomal recessive mutations.

Identification of *Bace2* Deletion Mutation as the Potential Causal Variation. To identify all possible autosomal recessive mutations in brown pandas, we conducted genome-wide screening and analysis of 35 deeply resequenced pandas on the basis of the recessive Mendelian inheritance pattern and geographic distribution of brown pandas. Specifically, we resequenced the whole genomes of two brown pandas (Dandan and Qizai) and four black pandas from two family trios associated with Qizai at a read depth of over 50× using the Illumina sequencing platform. In addition, we resequenced the whole genomes of 12 wild black pandas from the Qinling population and 17 wild black pandas from the non-Qinling population at a depth of over 30×, which were used as the

control to screen candidate mutations in population-level analysis (Dataset S4).

Furthermore, we sequenced and de novo assembled the chromosome-level genome of Xiyue, Qizai's father, using a combination of PacBio CLR, BioNano optical mapping, Illumina, and Hi-C techniques (*SI Appendix*, Table S2). The final genome assembly size was 2.47 Gb with a contig N50 of 9.25 Mb, which was about 72 times larger than that of the previous panda genome assembly (NCBI accession: GCF\_002007445.2) (12), and 124,613 (65%) of the previous genome gaps were filled. The BUSCO (13) complete score was 96%. The genome annotation pipeline identified a total of 18,999 protein-coding genes, 95.73% of which were functionally annotated (*SI Appendix*, Fig. S4 and Table S3).

We then called short and structural variants using our long-read-based genome assembly and population resequencing data (*SI Appendix*, Fig. S5). As a result, we detected a total of 18,147,295 short variants and 116,636 structural variants on autosomes. We determined that candidate variants *g* must meet these criteria: I) both the brown pandas Dandan and Qizai carry an identical homozygous variant *g*; II) at the family-trio level, the genotypes of B1 and B2 families follow a Mendelian inheritance pattern, as shown in Fig. 2*A*, and it is accepted that one of the parents in the B1 family or Zhuzhu in the B2 family has missing alleles; III) at the population level, none of the black Qinling and non-Qinling individuals should be

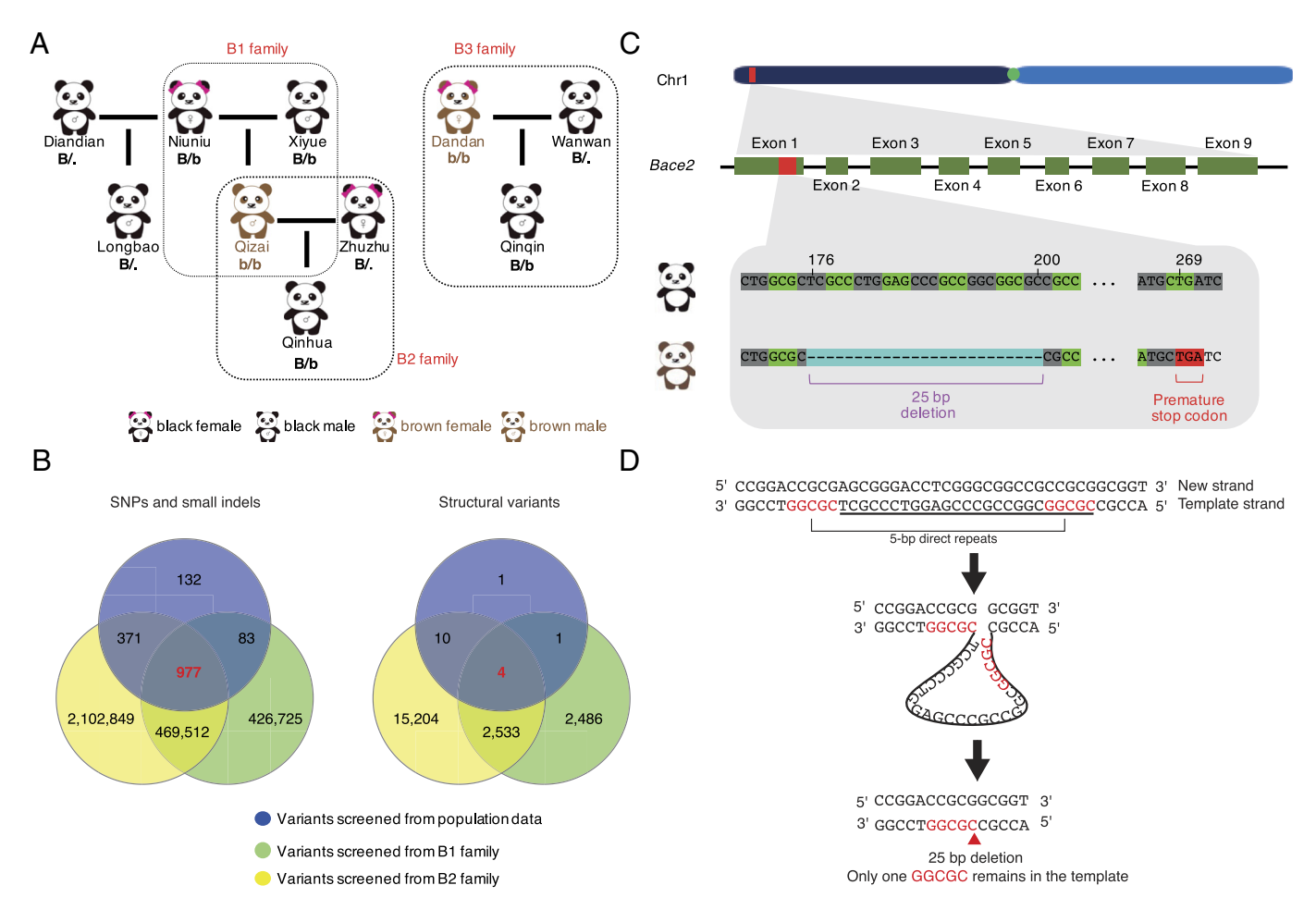


**Fig. 2.** Family trios of brown pandas and candidate *Bace2* deletion mutation. (*A*) Pedigrees of two brown pandas and their imputed genotypes. B represents the dominant allele, b represents the recessive allele, and the dot can be either B or b. (*B*) Venn diagram of candidate SNPs and small indels (*Left*) and structural variants (*Right*) obtained from genome resequencing data of the B1 family, the B2 family, and other Qinling and non-Qinling individuals. (*C*) Characterization of the wild-type and mutated *Bace2* genes. This gene is located on the reverse strand of Chr1 from 4467053 to 4546015 and contains 9 exons, which are marked in green. The 25-bp deletion c.176\_200del in the first exon, which occurs on 4545815 to 4545839, is highlighted in a light blue block. This deletion will result in a frameshift and a premature stop codon at the original nucleotide position 269 (marked in red). (*D*) DNA replication slippage may cause the 25-bp deletion in *Bace2*. The original template contains a direct repeat ("GGCGC," marked in red) that may cause replication slippage in the template strand (*Middle* figure) and result in a deletion (underlined in the *Top* figure) in the new strand that only keeps one "GGCGC" repeat.

homozygous for g; since brown pandas are endemic to the Qinling Mountains, we assumed that the non-Qinling population carried the mutation at a low frequency. The results showed that 977 short variants and four structural variants met the above screening criteria (Fig. 2B and Datasets S5 and S6). Among these variants, 650 were distributed in 38 identity-by-decent (IBD) segments shared between Qizai and Dandan (the two brown pandas), and only two IBD segments contained variants that occurred in protein-coding regions. One IBD segment (Chr11: 19539708-20712183) has a synonymous mutation (c.48C>T) in the DNAJC16 gene, and the other segment (Chr1: 4221483-4693914) possesses a 25-bp deletion (c.176\_200delTCGCCCTGGAGCCCGCCGGCGCGC) in the first exon of the Bace2 gene on Chr1 4545815 (Fig. 2C). This deletion occurs at a GC-rich region, containing 73.7% GC bases from 4545077 to 4547134, much higher than the 41.2% in the whole genome. Interestingly, the initial 185 bp of the first exon of the Bace2 gene within this GC-rich region, which is important for discovering this deletion, was missing in the previous short-read-based panda genome assembly, demonstrating the advantage of long-readbased genome assembly for the study of GC-rich regions (14). Moreover, the deletion is flanked by two repeat sequences (5-bp direct repeats "GGCGC") on both sides, which may induce DNA replication slippage in the template strand and further lead to the deletion (15) (Fig. 2D).

This deletion C.176\_200del results in a frameshift mutation in the first exon of the *Bace2* gene, leading to a premature stop codon and the consequent loss of function. Importantly, Bace2 was reported to be a pigmentation-related gene and encodes an aspartic protease that cleaves premelanosome protein (PMEL) into functional amyloids in melanocytes (SI Appendix, Fig. S6) (16). Several previous studies have established a link between the Bace2 gene and vertebrate coat pigmentation. In particular, Bace2 knockout can trigger PMEL misprocessing in mice, resulting in deficits in melanosome maturation. Consequently, this can lead to hair hypopigmentation (16, 17). These findings demonstrate that Bace2 mutation can influence pigmentation in vertebrates, and hence, the coat color variation in brown pandas may be attributable to the Bace2 deletion mutation.

Validation of the Bace2 Deletion in Brown Pandas Using DNA and RNA Sequencing Data. To verify the accuracy of the Bace2 deletion, we manually examined the genotypes of the Bace2 deletion by scrutinizing the read alignment of all resequenced panda individuals, including the B1 and B2 families, and resequenced Qinling and non-Qinling individuals (Fig. 3A). In family B1, due to the limitation of sequencing GC-rich regions with the short-read sequencing technique (18), Xiyue's genotype was missing at the locus, so we used its sequenced long reads and found a read depth pattern characteristic of a heterozygous variant, with approximately half read depth of the nondeletion regions (Fig. 3A, B1 family). The B1 and B2 families demonstrated complete Mendelian inheritance patterns for the Bace2 mutation, with Xiyue, Niuniu, and Qinhua identified as heterozygotes and Qizai as a homozygote. Read alignment analysis for the Qinling and non-Qinling populations revealed that except for Dandan and Qizai, which are homozygous mutants, all the other resequenced black pandas are homozygous wild types.

To investigate the structural integrity of the Bace2 gene, we performed RNA-seq analysis of hair samples from a black panda and Qizai (Fig. 3B). We identified 9 exons in Bace2 using a conventional gene annotation pipeline, which was confirmed by RNA-seq read alignment. Furthermore, RNA-seq read alignment detected a homozygous deletion in the first exon of Bace2 in Qizai,

while no deletion occurred in the black panda, confirming the presence of this deletion in brown pandas.

In addition, we assessed the degree of conservation of the protein-coding gene sequences and protein sequences surrounding the deletion of Bace2 among 13 Carnivora species (Fig. 3C, SI Appendix, Fig. S7, and Dataset S7). We found that the protein-coding gene sequence of Bace2 was highly conserved in Carnivora. All species, except for the brown panda and stoat, displayed the same protein

Validation of Bace2 Deletion Using PCR and Sanger Sequencing of 192 Black Pandas. To further reinforce the validity of the association between the Bace2 deletion and brown-and-white coat color, we sequenced the 25-bp deletion region in an additional cohort of 192 black pandas using PCR and Sanger sequencing. The cohort included 14 individuals with Qinling source, 177 individuals with non-Qinling source, and one hybrid between Qinling and non-Qinling pandas. The results showed that none of these black pandas were homozygous for the deletion mutation and that two pandas from the Qinling source were heterozygotes, which aligns with our screening criteria. Combined with 35 genomeresequenced individuals in this study, we generated a dataset of variant genotypes of 227 pandas, including 30 individuals with Qinling source, 194 individuals with non-Qinling source, and three hybrids (Fig. 3D and Dataset S8). The results showed that only two brown pandas were homozygous mutants (Dandan and Qizai), four black individuals from the Qinling source and one hybrid (Qinhua, i.e., Qizai's offspring) were identified as heterozygotes, and all the others were homozygous wild-type black pandas. Notably, none of the non-Qinling individuals carried this mutation, which coincided with the observation that brown pandas only occur in the Qinling Mountains.

Validation of the Bace2 Deletion Using Gene Knockout Mice. To validate the coat color effect of the Bace2 deletion, we took advantage of the CRISPR-Cas9 gene editing technique and removed the orthologous sequence of the deletion of the panda Bace2 gene in black C57BL/6J mice. The resulting 78 homozygous mutant mice all displayed light brown coat color compared with their wild-type counterparts. Regularly, mouse hair undergoes cycles of growth (anagen), regression (catagen), and rest (telogen) (19). We observed wild-type and homozygous mutant mice at the second anagen (5.1 to 5.4 wk old) and the third telogen (16 to 17 wk old) (Fig. 4A and SI Appendix, Fig. S8). Mutant mice in both periods exhibited lighter coat color compared to wild-type ones. Notably, the telogen mutant mice displayed lighter brown hairs in contrast to the anagen mutant mice. This observation suggests that the loss of pigmentation may intensify with time.

Cellular Basis for Hypopigmentation in Bace2<sup>-/-</sup> Mice. Hypopigmentation is often attributed to malfunctions in melanocyte proliferation and migration, melanosome biogenesis, melanin synthesis, and transfer (6, 20). In this study, we observed a reduction in both melanosome number and size in the hairs of the brown panda.

To determine whether the knockout mice displayed a melanosome pattern similar to that of the brown panda, we first examined the distribution of melanosomes in hairs of Bace2+/+ and Bace2-/mice at anagen and telogen under a microscope (Fig. 4B). We observed that the  $Bace2^{-1}$  mice at both periods exhibited fewer melanosomes than  $Bace2^{+1}$  mice. Additionally, we found that melanosome loss was greater at telogen, which corresponded to their lighter brown coat color than that of mutant mice at anagen.

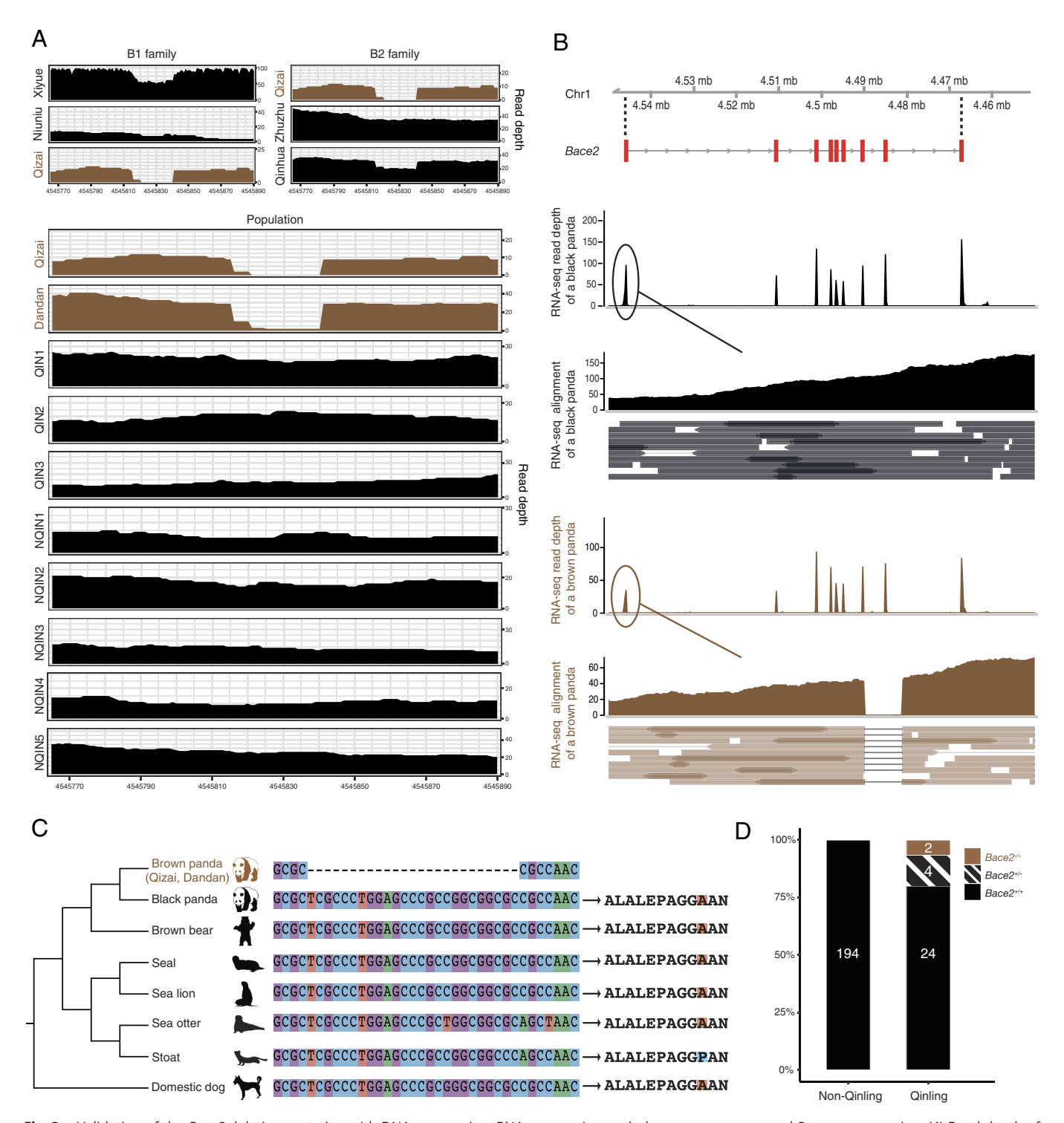


**Fig. 3.** Validation of the *Bace2* deletion mutation with DNA sequencing, RNA sequencing, orthologous sequences, and Sanger sequencing. (*A*) Read depth of short-read sequencing data around the deletion mutation for brown panda families B1 and B2 and a subset of Qinling and non-Qinling individuals. Individuals prefixed with QIN and NQIN are from Qinling and non-Qinling sources, respectively. (*B*) RNA-seq reads from the hair follicles of a black panda and a brown panda mapped onto the *Bace2* gene. The gene structure highlighted in red blocks is obtained from gene annotation pipeline, the first and second alignment track shows read coverage for each exon, reads that are mapped onto 1st exon are illustrated to show the deletion in the brown panda (blank region in the second alignment track). (*C*) Multiple sequence alignment of protein-coding sequences of seven Carnivora species around the deletion mutation. The deletion in the brown panda is shown as dashed lines. (*D*) The genotype distribution of the 25-bp deletion mutation for 224 giant pandas involved in this study, excluding three hybrids. Only two brown giant pandas (Qizai and Dandan) in the Qinling population were homozygous mutants (*Bace2*<sup>-/-</sup>), and four Qinling individuals were heterozygous carriers (*Bace2*<sup>-/-</sup>).

We then used TEM to conduct a detailed melanosome investigation in hairs (Fig. 4C). We quantified the melanosome number per pigment cell and found that, on average, the number of melanosomes in wild-type mice was 1.23 times that of the knockout mice (Fig. 4D and Dataset S9). Moreover, we analyzed the size distribution of

melanosomes in 1,029 and 3,198 melanosomes of  $Bace2^{+/-}$  and  $Bace2^{+/+}$  mice, respectively (Fig. 4E and Dataset S9). Wild-type mice had a significantly larger melanosome size (P < 0.001), which was 1.49 times that of the knockout mice on average. In summary, our findings suggest that knockout mice have fewer and smaller

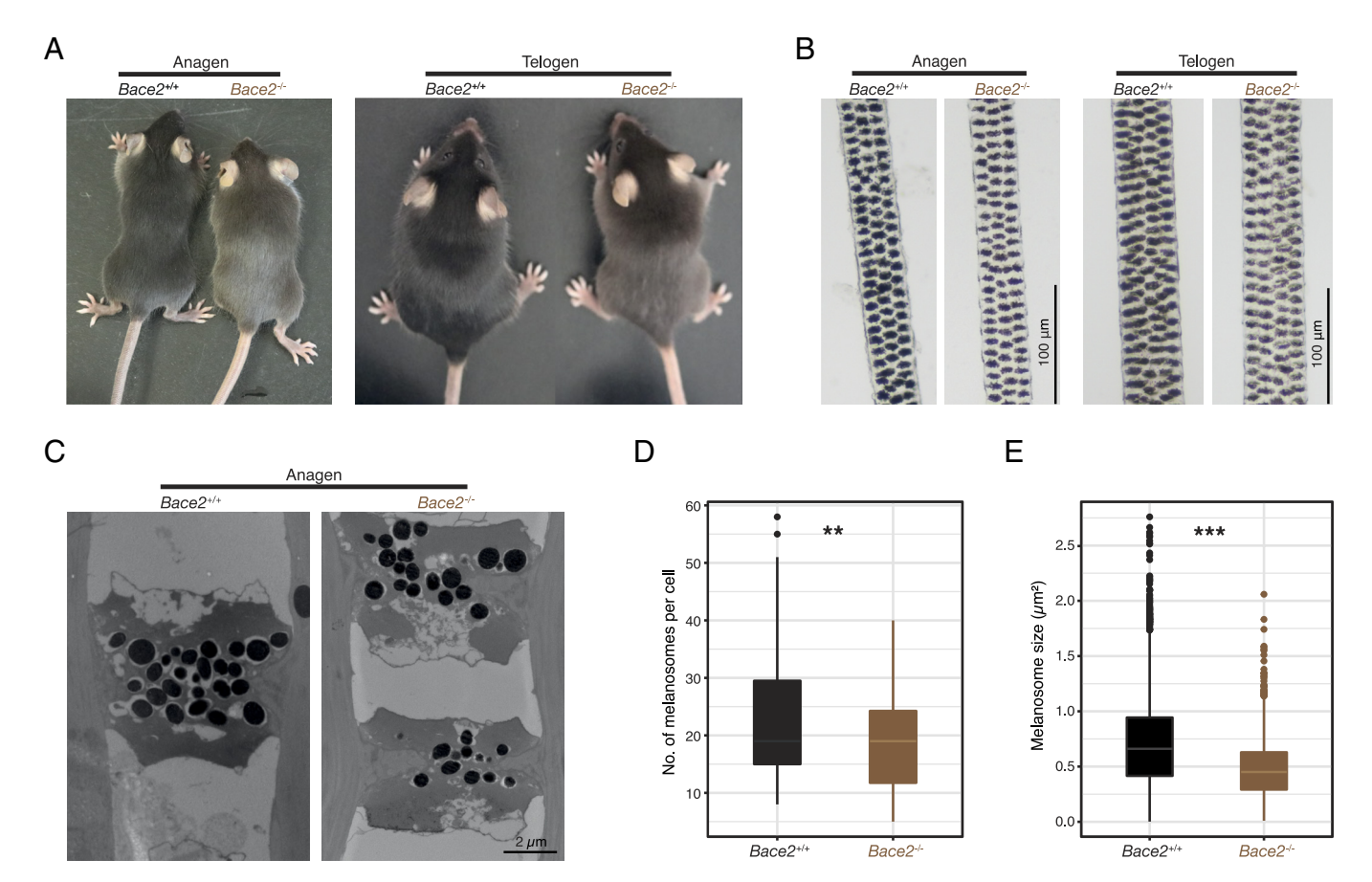


Fig. 4. Phenotypes of Bace2 knockout mice. (A) Photos of homozygous mutant and wild-type mice at anagen (Left) and telogen (Right). The mutant mouse shows a light brown coat color, while the wild-type mouse has a black coat color. (B) Micrographs of hairs of  $Bace2^{-/-}$  and  $Bace2^{+/+}$  mice at anagen and telogen. (C) TEM images of a longitudinal section of hairs from  $Bace2^{+/+}$  (Left) and  $Bace2^{-/-}$  mice (Right). (D) Melanosome number per pigment cell (100 cells for  $Bace2^{+/+}$  mice and 36 cells for  $Bace2^{-/-}$  mice,  $Bace2^{-/-}$  mice,  $Bace2^{-/-}$  mice,  $Bace2^{-/-}$  mice,  $Bace2^{-/-}$  mice and  $Bace2^{-/-}$ 

melanosomes than their wild-type counterparts, which is consistent with our observations in panda hair samples. These results support the notion that the *Bace2* deletion is most likely the genetic basis of the brown coat color in pandas.

### Discussion

Our study reveals that a homozygous 25-bp deletion in *Bace2*, a gene encoding protease-cleaving PMEL in melanocytes, most likely leading to hypopigmentation in brown pandas. Previous research has demonstrated the role of the Bace2 mutation in causing pigmentation variation in mice (16, 17). Here, our study presents that Bace2 mutation may cause coat color variation in wild animals. Using long-read-based panda genome and population resequencing data, we identified the deletion mutation of *Bace2* as the possible causal variant from genome-wide screening of short variants and structural variants at both the family-trio and population levels. We further validated this deletion through PCR and Sanger sequencing of an additional cohort of 192 black pandas and CRISPR-Cas9 knockout mice. All homozygous knockout mice exhibited a light brown coat color. TEM observation showed that the number and size of their melanosomes significantly decreased. These findings strongly support that this deletion of *Bace2* is most likely the genetic basis of brown-and-white coat color in brown pandas.

BACE2 has a vital role in cleaving PMEL to form functional amyloids to support the ellipsoidal shape of melanosomes in melanocytes (16, 21). The knockout of *Pmel* in mice has been proven

to alter melanosome shape and impair melanosome maturation (8). These studies suggest that the decreases of melanosome number and size in the brown panda and the *Bace2* knockout mice are likely triggered by PMEL misprocessing. There are, however, limitations in this study. Even though multiple lines of evidence support the *Bace2* deletion mutation as the genetic basis of brown coat color, only two brown pandas, available up to date, were involved in this study. It is necessary to sample more brown pandas in the future to confirm the reliability of this mutation. Additionally, further research is required to understand gene interactions and regulatory networks involved in this hypopigmentation process.

The brown panda is a rare natural coat color mutant discovered in the Qinling Mountains. The extremely low number of brown pandas and the nature of the frameshift deletion mutation suggest that this mutation could be a neutral or weakly deleterious mutation (22). Notably, two brown pandas (Qizai and Dandan) have exhibited normal growth and reproduction while the Bace2 knockout mice are viable, fertile, and do not have noticeable physical abnormalities, indicating that this mutation does not have obviously negative impacts on the fitness of these individuals. However, other physiological impacts of this mutation on the brown pandas remain unclear, as Bace2 is known to be involved in the Alzheimer's disease pathway (23, 24). Considering the small population size of the Qinling giant panda population, weakly deleterious mutations might be fixed due to the genetic drift effect. Thus, further studies on the brown panda and the knockout mouse model will provide valuable insights into the functional effects of this mutation. For

the rare coat color mutant of giant panda with great scientific and ornamental values, our findings would offer guidance on the scientific breeding of the brown pandas.

### **Materials and Methods**

A detailed description of computational and experimental methods applied in this study is provided in SI Appendix, Supporting Materials and Methods. Briefly, the identification of the pedigree for the brown panda Qizai was carried out by the paternity assignment method described in Hu et al. (11) using giant pandaspecific microsatellite loci. The chromosome-level genome assembly was created using a combination of sequencing data generated on PacBio Sequel, BioNano optical mapping, Illumina, and Hi-C technology. The short variants were called and genotyped using NGS reads of 35 genome-resequenced pandas with GATK (25), and SVs were identified and genotyped with Manta and Graphtyper (26). The candidate variants were screened by applying the rules derived from the inheritance pattern and geographic distribution of the brown pandas at both family and population levels. The 25-bp deletion of Bace2 and its functional effects were further validated by Sanger sequencing of another 192 black pandas and CRISPR-Cas9 knockout mice. The phenotypic features of the hairs from pandas and mice were observed using microscopy and TEM.

- H. E. Hoekstra, J. G. Krenz, M. W. Nachman, Local adaptation in the rock pocket mouse (Chaetodipus intermedius): Natural selection and phylogenetic history of populations. Heredity 94, 217-228 (2005).
- M. R. Jones et al., Adaptive introgression underlies polymorphic seasonal camouflage in snowshoe hares. Science 360, 1355-1358 (2018).
- E. E. Puckett et al., Genetic architecture and evolution of color variation in American black bears. Curr. Biol. 33, 86-97.e10 (2023).
- Y. Hu et al., Molecular mechanisms of adaptive evolution in wild animals and plants. Sci. China Life Sci. 66, 453-495 (2023).
- G. S. Barsh, What controls variation in human skin color? *PLoS Biol.* **1**, E27 (2003). H. E. Hoekstra, Genetics, development and evolution of adaptive pigmentation in vertebrates. Heredity 97, 222-234 (2006).
- H. Nicholls, Mystery of the brown giant panda deepens. Nature (2010), 10.1038/news.2010.19.
- A. R. Hellström et al., Inactivation of Pmel alters melanosome shape but has only a subtle effect on visible pigmentation. PLoS Genet. 7, e1002285 (2011).
- Z. Zhang et al., Ecological scale and seasonal heterogeneity in the spatial behaviors of giant pandas. Integr. Žool. **9**, 46–60 (2014).
- W. Wei et al., Hunting bamboo: Foraging patch selection and utilization by giant pandas and implications for conservation. Biol. Conserv. 186, 260-267 (2015).
- Y. Hu et al., Inbreeding and inbreeding avoidance in wild giant pandas. Mol. Ecol. 26, 5793-5806
- 12. H. Fan et al., Chromosome-level genome assembly for giant panda provides novel insights into Carnivora chromosome evolution. Genome Biol. 20, 267 (2019).
- 13. F. A. Simão, R. M. Waterhouse, P. Ioannidis, E. V. Kriventseva, E. M. Zdobnov, BUSCO: Assessing genome assembly and annotation completeness with single-copy orthologs. Bioinformatics 31, 3210-3212 (2015).
- 14. M. O. Pollard, D. Gurdasani, A. J. Mentzer, T. Porter, M. S. Sandhu, Long reads: Their purpose and place. Hum. Mol. Genet. 27, R234-R241 (2018).

Data, Materials, and Software Availability. The chromosome-level genome assembly and genome sequencing data of giant pandas in this study, including PacBio CLR, Illumina, Hi-C and population resequencing data, and RNA-seq data of panda hairs are available from the National Genomics Data Center, China (https://ngdc.cncb.ac.cn/), with project accession number PRJCA013191 (27).

ACKNOWLEDGMENTS. We thank the Foping and Changqing National Nature Reserves, Shaanxi for help with sample collection of wild giant pandas. We thank Shaanxi (Louguantai) Rescue and Breeding Center for Rare Wildlife, Chengdu Research Base of Giant Panda Breeding, China Research and Conservation Center for the Giant Panda, Beijing Zoo, and Chongqing Zoo for help with sample collection of captive giant pandas. We thank Ying Li and Wei Wan from Tsinghua University and Weiwei Zhai, Shuai Ma, Meng Wang, Huiwen Liu, and Kexin Li from Institute of Zoology, CAS, and Qi Wu from Institute of Microbiology, CAS, for their assistance in this study. This study was supported by the National Natural Science Foundation of China (31821001, 32100329), the Strategic Priority Research Program of Chinese Academy of Sciences (XDB31000000), the Major Program of the Natural Science Foundation of Jiangxi Province of China (20233ACB209001), and the Youth Innovation Promotion Association, CAS (Y202026).

- 15. M. Bzymek, S. T. Lovett, Instability of repetitive DNA sequences: The role of replication in multiple mechanisms. Proc. Natl. Acad. Sci. U.S.A. 98, 8319-8325 (2001).
- L. Rochin et al., BACE2 processes PMEL to form the melanosome amyloid matrix in pigment cells. Proc. Natl. Acad. Sci. U.S.A. 110, 10658-10663 (2013).
- D. R. Shimshek et al., Pharmacological BACE1 and BACE2 inhibition induces hair depigmentation by inhibiting PMEL17 processing in mice. Sci. Rep. 6, 21917 (2016).
- D. Aird et al., Analyzing and minimizing PCR amplification bias in Illumina sequencing libraries. Genome Biol. 12, R18 (2011).
- L. Alonso, E. Fuchs, The hair cycle. *J. Cell Sci.* **119**, 391–393 (2006).

  B. Zhang *et al.*, Hyperactivation of sympathetic nerves drives depletion of melanocyte stem cells. Nature 577, 676-681 (2020).
- 21. B. Watt, G. van Niel, G. Raposo, M. S. Marks, PMEL: A pigment cell-specific model for functional amyloid formation. Pigment Cell Melanoma Res. 26, 300-315 (2013).
- J. Robinson, C. C. Kyriazis, S. C. Yuan, K. E. Lohmueller, Deleterious variation in natural populations and implications for conservation genetics. Annu. Rev. Anim. Biosci. 11, 93-114 (2023).
- Z. Wang et al., BACE2, a conditional  $\beta$ -secretase, contributes to Alzheimer's disease pathogenesis. JCI Insight 4, e123431 (2019).
- I. Alić et al., Patient-specific Alzheimer-like pathology in trisomy 21 cerebral organoids reveals BACE2 as a gene dose-sensitive AD suppressor in human brain. Mol. Psychiatry 26, 5766–5788
- 25. A. McKenna et al., The Genome Analysis Toolkit: A MapReduce framework for analyzing nextgeneration DNA sequencing data. Genome Res. 20, 1297-1303 (2010).
- H. P. Eggertsson et al., GraphTyper2 enables population-scale genotyping of structural variation using pangenome graphs. Nat. Commun. 10, 5402 (2019).
- 27. D. Guan et al., Taking a color photo: A homozygous 25-bp deletion in Bace2 may cause brown-andwhite coat color in giant pandas. National Genomics Data Center, China. https://ngdc.cncb.ac.cn/ bioproject/browse/PRJCA013191. Deposited 14 November 2022.